Research in Pharmaceutical Sciences, October 2024; 19(5): 606-621
Received: 21-05-2024
Peer Reviewed: 23-06-2024
Revised: 02-08-2024
Accepted: 21-08-2024
Published: 22-10-204

School of Pharmacy & Pharmaceutical Sciences
Isfahan University of Medical Sciences

Original Article

The activation of the G-protein-coupled estrogen receptor promotes the aggressiveness of MDA-MB231 cells by targeting the IRE1α/TXNIP pathway

Maryam Mohammad-Sadeghipour[1], Mohammad Hadi Nematollahi[2], Hassan Ahmadinia[3], Mohammad Reza Hajizadeh[4,5,*], and Mehdi Mahmoodi[1,4,*]

[1]*Department of Clinical Biochemistry, Afzalipoor Faculty of Medicine, Kerman University of Medical Sciences, Kerman, Iran.*
[2]*Applied Cellular and Molecular Research Center, Kerman University of Medical Sciences, Kerman, Iran.*
[3]*Department of Epidemiology and Biostatistics, School of Health, Occupational Environment Research Center, Rafsanjan University of Medical Sciences, Rafsanjan, Iran.*
[4]*Molecular Medicine Research Center, Institute of Basic Medical Sciences Research, Rafsanjan University of Medical Sciences, Rafsanjan, Iran.*
[5]*Department of Clinical Biochemistry, Faculty of Medicine, Rafsanjan University of Medical Sciences, Rafsanjan, Iran.*

Abstract

Background and purpose: This study investigated modulating the G protein-coupled estrogen receptor (GPER) on the IRE1α/TXNIP pathway and its role in drug resistance in MDA-MB231 cells.
Experimental approach: To determine the optimal concentrations of G_1 and 4-hydroxytamoxifen (TAM), GPER expression and ERK1/2 phosphorylation were analyzed using qRT-PCR and western blotting, respectively. Cells were treated with individual concentrations of G_1 (1000 nM), G_{15} (1000 nM), and TAM (2000 nM), as well as combinations of these treatments (G_1 + G_{15}, TAM + G_{15}, and G_1 + TAM) for 24 and 48 h. The expression levels of GPER, IRE1α, miR-17-5p, TXNIP, ABCB1, and ABCC1 genes and TXNIP protein expression were evaluated. Finally, apoptosis and cell migration were examined using flow cytometry and the wound-healing assay, respectively.
Findings/Results: Activating GPER with its specific agonist G_1 and TAM significantly increased IRE1α levels in MDA-MB231 cells. IRE1α through splicing XBP1 led to unfolded protein response. In addition, decreased TXNIP gene and protein expression reduced apoptosis, increased migration, and upregulated the genes associated with drug resistance.
Conclusion and implication: Our investigation revealed that blocking the GPER/IRE1α/TXNIP pathway in MDA-MB231 cells could enhance treatment efficacy and improve chemotherapy responsiveness. The distinct unfolded protein response observed in MDA-MB231 cells may stem from the unique characteristics of these cells, which lack receptors for estrogen, progesterone, and HER2/neu hormones, possessing only the GPER receptor ($ER^-/PR^-/HER2^-/GPER^+$). This study introduced a new pathway in TNBC cells, indicating that targeting GPER could be crucial in comprehensive therapeutic strategies in TNBC cells.

Keywords: Breast cancer; Drug resistance; G protein-coupled estrogen receptor; miR-17-5P; Thioredoxin interacting protein; Unfolded protein response.

INTRODUCTION

Triple-negative breast cancer (TNBC) or MDA-MB231 cells exhibit a feature called epithelial-to-mesenchymal transition, which is linked to the capacity of cancer cells to spread and infiltrate nearby tissues (1). The clinicopathological features of these cells are subtype B, lacking estrogen receptor (ER^-), progesterone receptor (PR^-), and Erb-B2 receptor tyrosine kinase/human epidermal growth factor receptor 2 ($ERBB2/HER2^-$) expression.

*Corresponding authors:
M. Mahmoodi, Tel: +98-9131914855, Fax: +98-3433257671
Email: me.mahmoodi@kmu.ac.ir
M.R. Hajizadeh, Tel: +98-3431315023, Fax: +98-3431315003
Email: dr.hajizadeh@rums.ac.ir

Access this article online	
	Website: http://rps.mui.ac.ir
	DOI: 10.4103/RPS.RPS_96_24

The source is pleural effusion, and the tumor type is metastatic adenocarcinoma. *In vitro*, MDA-MB-231 cells attach to the culture surface and grow as a monolayer (2). Despite advancements in treatments like poly-ADP-ribose polymerase inhibitors and immunotherapy, the prognosis for TNBC remains markedly inferior compared to that for non-TNBC (3). The primary causes of death are recurrence and distant metastasis (4). Consequently, they have not been very successful in treating TNBC. To address these issues, researchers have turned to targeting estrogen receptors as a potential treatment for breast cancer (5). One such receptor is the G-protein-coupled estrogen receptor (GPER) also known as GPER1 or GPR30, located in the cell membrane and the endoplasmic reticulum (ER). GPER has different functions than the classic nuclear estrogen receptors (ER-α and ER-β) (6). G_1 is a selective agonist of GPER, while 4-hydroxytamoxifen (TAM) is a selective ER modulator that acts as an antagonist of the ER but an agonist of GPER. Recent studies have shown that G_1 and TAM exhibit a strong binding affinity t GPER. G_1 has been found not to affect ERα/β at concentrations up to 10 μM (7). Therefore, in this study, both G_1 and TAM were used as GPER agonists. Additionally, G_{15} was used as a selective antagonist for GPER. Some studies have reported that disturbances in GPER expression can lead to the development of cancer by promoting the proliferation, migration, and invasion of breast cancer cells (8-10). On the other hand, several studies have suggested that GPER may act as a tumor suppressor and induce apoptosis (11-13). These contradictory findings suggest that GPER may be involved in complex pathways, and a better understanding of its role in breast cancer could be beneficial for future disease management and prevention. Additionally, GPER triggers the unfolded protein response (UPR) by inducing ER stress in breast cancer cells (12). ER stress occurs when the cell's demand for folding proteins exceeds the capacity of the organelle. This leads to a disruption of homeostasis in the ER, resulting in the accumulation of misfolded proteins and triggering the activation of defense mechanisms such as UPR (14). While UPR is typically inactive in healthy cells, it is activated in stressed cells and many types of tumor cells. The UPR is mediated by three molecular sensors located on the ER membrane: pancreatic endoplasmic reticulum kinase, activating transcription factor 6, and inositol-requiring enzyme 1 (IRE1) (15). When cells experience ER stress, IRE1α becomes activated and can process mRNA through unconventional splicing, specifically targeting the mRNA for X-box binding protein-1 (XBP1). The activation of XBP1 results in ER homeostasis by reducing ER protein loading and promoting the expression of chaperones that enhance protein folding capacity (16). Moreover, the endoplasmic-reticulum-associated protein degradation (ERAD) pathway, activated by XBP1, identifies and polyubiquitinates unfolded proteins, ultimately leading to their degradation in the proteasome (17). IRE1α can also degrade specific mRNAs or pre-miRNAs through a process known as regulated IRE1α-dependent decay (RIDD). The function of IRE1α can shift depending on the duration and type of ER stress, with acute stress leading to XBP1 splicing and chronic stress or over-expression leading to RIDD activity (18). Thioredoxin interacting protein (TXNIP) is one of the downstream targets of IRE1α, a potent tumor suppressor that is downregulated in breast cancer. This decrease in expression is associated with increased proliferative activity and estrogen-dependent growth, leading to worsened conditions in breast cancer cells (19). The GPER/IRE1α/TXNIP pathway has not been studied in breast cancer so far. Therefore, the current study aimed to demonstrate the effects of blocking or enhancing GPER on the IRE1α/TXNIP signaling pathway. Moreover, the role of GPER in breast cancer cell migration, apoptosis, and chemotherapy resistance in the MDA-MB231 cell line was determined.

MATERIALS AND METHODS

Reagents

The MDA-MB231 cell line was purchased from the Pasteur Institute (Iran, Tehran).

DMEM high glucose (4.5 g/L) powder medium (Dulbecco's modified eagle medium) and the fetal bovine serum (FBS) were acquired from Biosera (France). Penicillin/streptomycin and trypsin/ethylene diamine tetra acetic acid (EDTA) 0.25% were purchased from Bioidea/Idezist Notarkib (Iran, Tehran). Dimethyl sulfoxide (DMSO) was obtained from Merck (USA), 3-(4,5-dimethylthiazol-2-yl)-2,5-diphenyltetrazolium bromide (MTT) was purchased from Sigma (Sigma-Aldrich, USA) for cell culture. TRIzol reagent was purchased from Invitrogen (Thermo Fisher Scientific, USA), cDNA synthesis kit from PARS Tous (Iran, Mashhad), Bon stem high sensitivity MicroRNA 1st strand cDNA synthesis kit and Bon high specificity quantitative real-time polymerase chain reaction (qRT-PCR) master mix from Bon yakhteh (Iran, Tehran), which were all prepared. GPER-specific agonist G1 (3577, purity ≥ 98%, molecular weight of 412.28) from Tocris (Ellisville, MO, USA) and G15 as a well-established antagonist of GPER (HY-103449, purity ≥ 99.0%, molecular weight of 370.24) from Med Chem Express (USA) were purchased. TAM was obtained from Hello Bio (HB6040, USA, purity ≥ 98%, molecular weight of 387.52). Antibodies used in western blotting were anti-pancreatic endoplasmic reticulum kinase (p-ERK1/2; 9101, 1:1000), anti-ERK1/2 (4696, 1:2000), anti-rabbit (7074, 1:2500), and anti-mouse (7076, 1:2500) horseradish peroxidase (HRP)-conjugated secondary antibodies were bought from Cell Signaling Technology Inc. (USA). Anti-TXNIP (STJ113636, 1:2000) and anti-β-actin (Sc-47778, 1:4000) were purchased from St John's Laboratory Ltd (London) and Santa Cruz Biotechnology (CA, USA), respectively. One mg of G1, G15, and TAM were dissolved in 2.43, 5.4, and 0.5 mL DMSO to prepare 1, 0.5, and 5 mM stock solutions, respectively. These solutions were then added to the medium at the indicated concentrations. The stocks of G1 and G15 were stored in the dark at -20°C for subsequent experiments, except for TAM which had to be freshly prepared before each test.

Cell culture

The MDA-MB231 cell line was maintained in DMEM high glucose supplemented with 10% FBS, 100 U/mL penicillin, and 10 mg/mL streptomycin at 37 ℃ in a 5% CO_2 atmosphere. Before the experiments, all cells were transferred to the FBS- and phenol-free medium for 24 h.

Evaluating the cytotoxic effects of G_1, TAM, and G_{15} by the MTT assay

To determine the cytotoxic effects of G_1, G_{15}, and TAM, cells were seeded into each well of a 96-well plate in 100 µL of medium supplemented with 10% FBS. Once the cells reached 70-80% confluency, the medium was replaced with 100 µL of FBS- and phenol-free medium for another 24 h. Various concentrations of G_1 and G_{15} (0- 0.001- 0.01- 0.1- 1- 2.5- 5- 10 µM), and TAM (0- 0.01- 0.1- 1- 2- 4- 8- 16- 32- 64 µM) were added to three replicate wells for each treatment. After incubation for 24 and 48 h, the 5 mg/mL MTT solution was added to each well and incubated for an additional 4 h. The medium was then removed and DMSO was added to each well. The plates were shaken on a rotator for 15 min and the absorbance was recorded at 570 nm using an ultraviolet spectrophotometric reader. The IC_{50} was calculated with probit regression analysis.

Determining the optimal concentration of GPER agonists (G_1 and TAM) in MDA-MB231 cells

Studies have reported that estrogen, G_1, or TAM can activate ERK or Akt through GPER/EGFR signaling in tumor cells (20, 21). To determine the optimal concentrations of G_1 and TAM by assessing GPER expression and the rapid activation of ERK1/2, first, the IC_{50} values of G_1 and TAM were calculated. Based on these results, the cells were treated with concentrations less than the IC_{50} of G_1 and TAM. Specifically, MDA-MB231 cells were exposed to G_1 at 10, 100, and 1000 nM, and TAM at 100, 1000, and 2000 nM for 12 h, then the GPER expression was evaluated using qRT-PCR. In addition, western blotting techniques were used to assess the phosphorylation of ERK1/2.

The concentrations of G_1 and TAM that resulted in the highest levels of GPER expression and ERK1/2 phosphorylation were selected for subsequent experiments. This approach allowed us to use concentrations with lower cytotoxicity while providing the highest level of GPER stimulation.

Western blot analysis

To determine the optimal concentration of G_1 and TAM, MDA-MB231 cells were grown to 60-70% confluency in 10% FBS medium. After this, 100 µL of medium (without FBS and phenol red) containing G_1 (0, 10, 100, and 1000 nM) and TAM (0, 100, 1000, and 2000 nM) was added to the cells. The cells were incubated with G_1 for 30 min (21,22) and with TAM for 5 min (23). They were then trypsinized, washed with cold PBS, and lysed with cell lysis buffer (20 mM Tris, pH 7.5, 15 mM KCl, 1% CHAPS, 5 mM $MgCl_2$, 1 mM EDTA, 1 mM EGTA CPIM, and protease/phosphatase inhibitor). The lysed cells were collected using a scraper and kept on ice for 30 min. Protein concentrations were measured using the detergent-compatible (DC) kit (Bio-Rad, USA). The cell lysate was boiled at 95 °C for 5 min and 50 µg of protein per lane was electrophoresed on a 12.5% sodium dodecyl-sulfate polyacrylamide gel electrophoresis (SDS-PAGE) and electroblotted onto polyvinylidene difluoride (PVDF) membranes (0.45 µm pore size, Millipore, USA). The membrane was then blocked with 5% non-fat dry milk in tris-buffered saline and 0.1% tween-20 (TBST) for 20-40 min at room temperature. Next, the membrane was incubated with primary anti-p-ERK1/2 (1:1000) and primary anti-ERK1/2 (1:2000) diluted in tris-buffered saline-milk-tween-20 at 4 °C overnight. After being washed with TBST buffer, the membrane was incubated with anti-rabbit and anti-mouse HRP-conjugated secondary antibodies. Protein bands were visualized using ECL and Kodak X-OMAT LS film. The data was quantified using ImageJ software. Beta-actin was used as an internal control to normalize the results (24).

The following step involved exposing cells to G_1 (1000 nM), G_{15} (1000 nM), and TAM (2000 nM) individually, or a combination of G_1 + G_{15} (1000 nM, 1000 nM), TAM + G_{15} (2000 nM, 1000 nM), and G_1 + TAM (1000 nM, 2000 nM) for 24 and 48 h to evaluate the level of TXNIP protein expression. Before this, the cells were pre-treated with G_{15} for 1 h (25). To measure the amount of TXNIP protein, we used the western blot technique mentioned above, using anti-TXNIP, anti-rabbit IgG, and HRP-conjugated secondary antibodies. All the experiments were added to tree replicate wells for each treatment. Untreated cells were considered the control.

qRT-PCR

The total RNA was isolated from cultured cells using the TRIzol® reagent according to the manufacturer's instructions. The quantity and quality of RNA samples were analyzed using a Nanodrop (model: DS-11 FX+ Spectrophotometer/Fluorometer, USA) and 1.5% agarose gel electrophoresis, respectively.

The complementary DNA (cDNA) was synthesized employing a Pars Tous kit (Iran) according to the manufacturer's instructions. To remove DNA contamination, RNA was treated with the enzyme DNase I. Briefly, 3-5 µg of pure mRNA, oligo dT, random hexamer, and reverse transcriptase enzymes were used to synthesize cDNA in a final volume of 20 µL. Reverse transcription reaction was performed at 37 °C for 60 min and 95 °C for 5 min by a Thermal Cycler (Bio-Rad, California, USA). cDNA synthesis for microRNA was done in two steps. In this experiment, a Bon Stem High Sensitivity microRNA First Strand cDNA synthesis kit was used. In the first step, with the assistance of the A polymerase enzyme, multiple A nucleotides were added to the ends of small RNAs. In the second step, the synthesis of the first strand cDNA was carried out by following the specific instructions provided by the desired kit. The expression of the GPER, IRE1α, miR-17-5P, TXNIP, ATP binding cassette subfamily B member 1 (ABCB1), and ATP binding cassette subfamily C member 1 (ABCC1) genes was determined by qRT-PCR on an Applied Biosystems Step One Plus™ system (ABI, USA). The Bon high-specificity qRT-PCR master mix was used for these purposes. Gene expression was calculated using the formula $2^{(-\Delta\Delta Ct)}$. U6 and β-actin were used as internal references for miR-17-5p and other genes, respectively (26). The gene-specific primers are listed in Table 1.

Table 1. Nucleotide sequence of primers used in this study.

Gene	Forward sequence (5′ > 3′)	Reverse sequence (5′ > 3′)
GPER (NM_001039966.2)	ACTCCTCACACAGAATTGCTAC	GATTTGCTTTAGGGTTCCTGTG
IRE1α (NM_001433.5)	TCAAACACCCGTTCTTCTGGAG	GAATTTACGCAGGTCTGTCTGG
TXNIP (NM_001313972.2)	CTGATTTAATGGCACCTGTGTC	CATTGGCAAGGTAAGTGTGG
ABCB1 (MDR 1) (NM_000927.5)	AGAAGGTTCTGGGAAGATCG	GTTTATGTGCCACCAAGTAGG
ABCC1 (MRP 1) (NM_004996.4)	TCAGCCAGAAAATCCTCCAC	ATCGCCATCACAGCATTGAC
β-actin (NM_001101.5)	GGCATGGGTCAGAAGGATTCC	GATAGCACAGCCTGGATAGCA
Mir-17-5p (MIMAT0000070)	CAAAGTGCTTACAGTGCAG	
U6 (NR_004394.1)	CGCTTCGGCAGCACATATAC	AAATATGGAACGCTTCACGA

Apoptosis analysis by flow cytometry

The annexin V-phycoerythrin (PE)/propidium iodide (PI) apoptosis detection kit (Padzaco, Tehran, Iran) was used to assess cell apoptosis. The cells were seeded at a density of 10^5-10^6 per well on six-well plates and grown to 60-70% confluency. Cells pre-treated with G_{15} for 1 h and then treated with G_1 (1000 nM), G_{15} (1000 nM), and TAM (2000 nM) individually, or the combination of G_1 + G_{15} (1000 nM, 1000 nM), TAM + G_{15} (2000 nM, 1000 nM), and G_1 + TAM (1000 nM, 2000 nM). After 48 h, the cells were trypsinized, washed with PBS buffer, and resuspended in 100 µL binding buffer. They were then stained with 1 µL annexin V-fluorescein isothiocyanate (FITC) for 15 min and 1 µL PI for 5 min in a dark place at room temperature. Finally, 400 µL binding buffer was added and the cells were analyzed using a flow cytometer (BD Biosciences) within 1 h after the reaction was halted.

Cell migration analysis (wound-healing assay)

MDA-MB231 cells were cultured in a 6-well plate and allowed to a confluent cell monolayer. The cells were scratched with a 200 µL sterile pipette tip. Cells were then washed twice with PBS and treated with an FBS- and phenol-free medium containing either G_1 (1000 nM), G_{15} (1000 nM), and TAM (2000 nM) individually, or the combination of G_1 + G_{15} (1000 nM, 1000 nM), TAM + G_{15} (2000 nM, 1000 nM), and G_1 + TAM (1000 nM, 2000 nM) for 24 h. Photographs were taken exactly after scratching the cell layer (0 h) and 24 h later to assess scratch closure as an indication of cellular migration. Gap distances were analyzed using Image J software. Each experiment was validated three times.

Statistical analysis

The statistical analysis was performed by Graph Pad Prism 10.1 (Graph Pad Software, Inc.). Two-way ANOVA and one-way ANOVA followed by Dunnett's post hoc test were used to assess the differences among groups. Tukey's post hoc test was used to evaluate the differences between the combined treatment groups and the single treatment groups. Data were expressed as mean ± SD of at least three independent experiments unless otherwise specified. The *P*-values < 0.05 were considered statistically significant.

RESULTS

The cytotoxic effects of G_1, TAM, and G_{15} on MDA-MB231 cells

The cytotoxic effects of G_1, TAM, and G_{15} were evaluated by MTT test. The results indicated that concentrations of ≥ 0.01 µM of G_1 at 24 and 48 h, ≥ 0.01 µM of TAM at 24 h ≥ 1 µM of TAM at 48 h, and ≥ 0.01 µM of G_{15} at 24 h, and ≥ 0.001 µM of G_{15} at 48 h were significantly different from the control group. The IC_{50} values were calculated after 24 and 48 h of treatment with the aforementioned compounds and are shown in Fig. 1A-C.

Evaluating the optimal concentration of GPER agonists G_1 and TAM in MDA-MB231 cells

A study has reported that GPR30/EGFR signals rapidly activate ERK1/2 and cause its nuclear translocation. They discovered that G1 induced a rapid (within 15-30 min) phosphorylation of ERK1/2 in breast cancer cell lines (21).

Our study in MDA-MB231 cells showed that exposure to G1 at 100 and 1000 nM caused an increase in GPER expression and ERK1/2 phosphorylation. Furthermore, the concentrations of 100, 1000, and 2000 nM of TAM enhanced GPER expression and ERK1/2 phosphorylation (Fig. 2A-D). These findings suggest that the optimal concentrations for stimulating the highest GPER expression and ERK1/2 phosphorylation are 1000 nM for G1 and 2000 nM for TAM. Previous studies have shown that treatment with G15 at 1000 nM for 48 h inhibits the response of GPER to E2 and G1 in A549 and H1793 cell lines (27). Therefore, for the next experiments, G1 at 1000 nM and TAM at 2000 nM as selective GPER agonists, and G15 at 1000 nM as a GPER antagonist were used.

Investigating the induction or inhibition of GPER

To determine GPER induction or inhibition in MDA-MB231 cells, the GPER expression after treating the cells with 1000 nM of G_1, 2000 nM of TAM, and 1000 nM of G_{15} for 24 and 48 h was examined. The mRNA expression of GPER significantly increased after 24- and 48-h treatment with G_1 and/or TAM compared to the control group. Additionally, the results revealed that G_{15} effectively reversed the increasing effects of G_1 and TAM on GPER expression. For further confirmation, MDA-MB231 cells were pre-treated with G_{15} for 1 h and then with G_1 and TAM. In this regard, G_{15} significantly blocked G_1 and TAM-induced GPER upregulation (Fig. 3A). In addition, the induction of GPER in cells exposed to concurrent treatment with both G1 and TAM for 48 h was markedly elevated compared to treatments administered with either agent alone. The two-way ANOVA analysis revealed a significant difference in GPER gene expression in the G_1 + TAM group at 24 h compared to 48 h in MDA-MB231 cells (Fig. 3A).

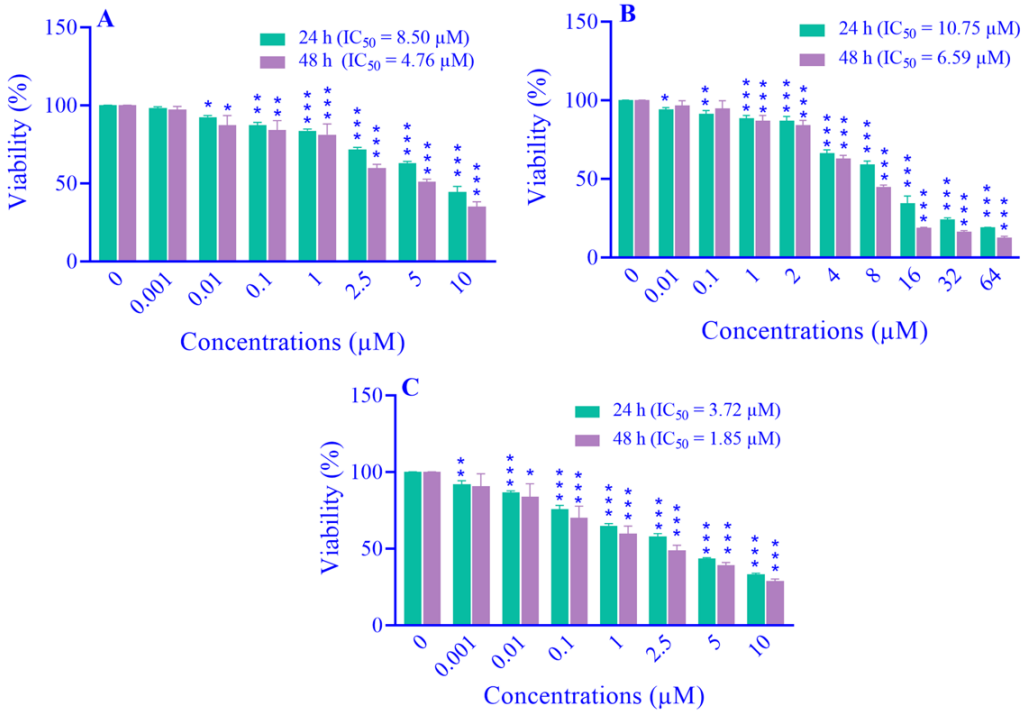

Fig. 1. The percentage of viable MDA-MB231 cells after 24 and 48 h of treatment with (A) G_1, (B) tamoxifen (TAM), and (C) G_{15} was evaluated using the MTT assay at various concentrations. The data are presented as mean ± SD, n = 3. *$P < 0.05$, **$P < 0.01$, and ***$P < 0.001$ indicate significant differences compared to the control group (concentration zero).

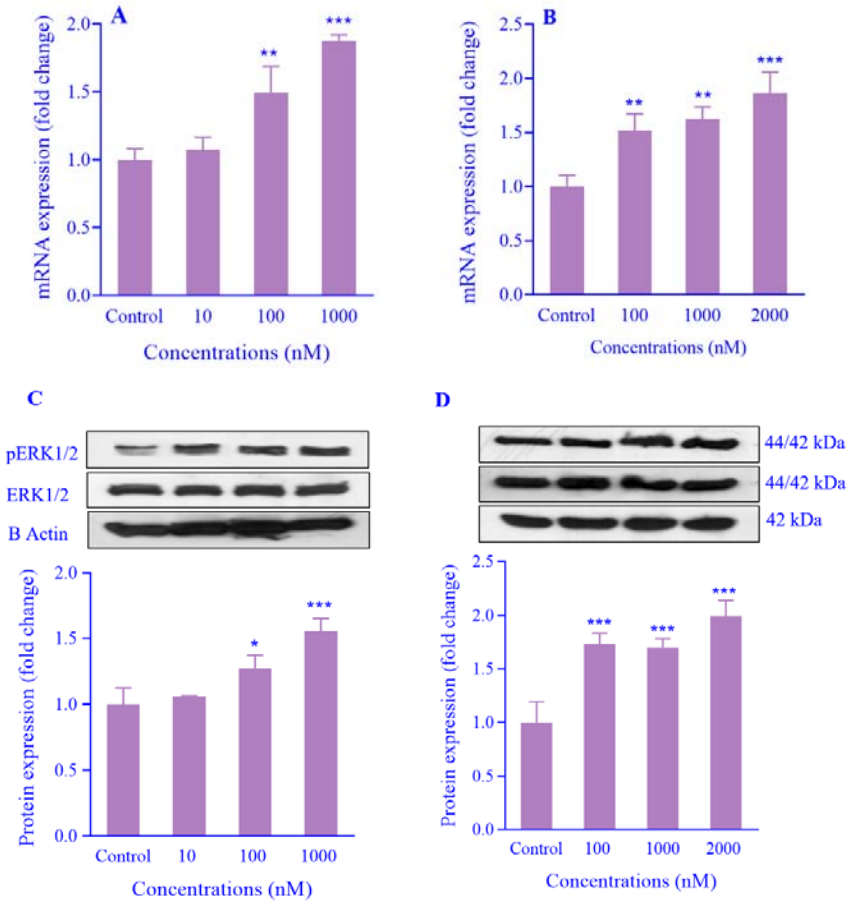

Fig. 2. G_1 and TAM induce mRNA gene expression of GPER and phosphorylation of ERK1/2 in the MDA-MB231 cell line. GPER mRNA expression of the cells treated with (A) G_1 (0, 10, 100, and 1000 nM) or (B) with TAM (0, 100, 1000, and 2000 nM) for 12 h was evaluated by qRT-PCR; and the ERK1/2 phosphorylation in the cells treated with (C) G_1 (0, 10, 100, and 1000 nM) for 30 min or (D) with TAM (0, 100, 1000, and 2000 nM) for 5 min was also evaluated using western blotting. The data represents the mean ± SD, n = 3. *$P < 0.05$, **$P < 0.01$, and ***$P < 0.001$ indicate significant differences compared to the control group. GPER, G-protein-coupled estrogen receptor; ERK, endoplasmic reticulum kinase; TAM, tamoxifen.

The effect of GPER induction or inhibition on IRE1α mRNA expression

To understand the relationship between GPER induction and UPR and its key sensor IRE1α, the mRNA gene expression of IRE1α was investigated after GPER induction with G_1 and TAM at 24 and 48 h. The results revealed that the induction of GPER by G_1 and TAM can up-regulate the expression of IRE1α in MDA-MB231 cells in comparison with the control group (Fig. 3B). To determine whether the up-regulation of IRE1α is stimulated by GPER induction signaling, the GPER-specific antagonist, G_{15}, was used. A significant reduction in IRE1α gene expression was observed when cells were treated with G_{15}. Additionally, the gene expression of IRE1α significantly decreased during the pre-treatment with G_{15} (G_1 + G_{15}, at 24 and 48 h compared to G_1 group; TAM + G_{15}, at 24 and 48 h compared to TAM group). Moreover, the combination treatment of G_1 and TAM resulted in increased expression of IRE1α in the cells at 24 and 48 h compared to cells treated merely with G_1 and cells exposed to TAM. Moreover, there was a significant variation in the gene expression of IRE1α that notably increased in both TAM and G_1 + TAM groups after 48 h compared to recorded expression after 24-h exposure (Fig. 3B).

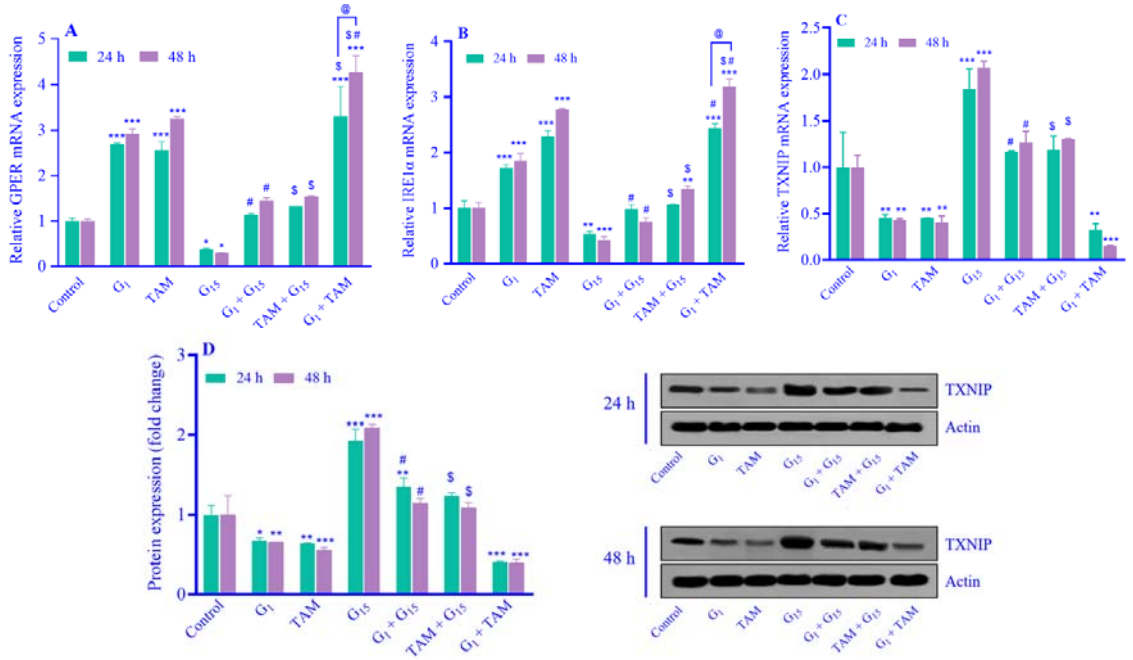

Fig. 3. Evaluating the effect of G_1 and TAM (as GPER agonists) and G_{15} (as a GPER antagonist) on the gene expression of (A) GPER, (B) IRE1α, (C) TXNIP, and (D) TXNIP protein expression after 24 and 48 h of treatment in the MDA-MB231 cells. The data represent means ± SD, n = 3. $^{*}P < 0.05$, $^{**}P < 0.01$, and $^{***}P < 0.001$ indicate significant differences compared to the control group; $^{\#}P < 0.05$ against G_1 group; $^{\$}P < 0.05$ versus TAM group; and $^{@}P < 0.05$ indicate significant differences between the designated groups. TAM, Tamoxifen; GPER, G-protein-coupled estrogen receptor; IRE, inositol-requiring enzyme; TXNIP, thioredoxin interacting protein.

The effect of GPER induction or inhibition on TXNIP mRNA expression

To confirm the GPER/IRE1α/TXNIP signaling pathway in MDA-MB231 cells, the mRNA and protein expression of TXNIP was assessed after 24 and 48 h of treatment with G_1, TAM, and G_{15}. This was done using qRT-PCR for mRNA analysis and western blotting for protein analysis. qRT-PCR analysis revealed that treatment with G_1 and TAM decreased the gene expression of TXNIP in MDA-MB231 cells after 24 and 48 h. As expected, G_{15} induced the expression of the TXNIP gene after 24 and 48 h. Pre-treatment of the cells with G_{15} (G_1 + G_{15} and TAM + G_{15}) reversed the G_1/TAM-induced reduction in TXNIP gene expression compared to the G_1 and TAM groups. However, there was no significant difference in the G_1 + TAM group compared to the G_1 and TAM groups separately (Fig. 3C). Western blot analysis revealed a significant decrease in TXNIP protein expression in MDA-MB-231 cells after 24- and 48-h treatment with G_1 and TAM compared to the respective control group. Additionally, blocking GPER using G_{15} significantly increased the expression of TXNIP protein in MDA-MB-231 cells. Furthermore, in the G_1 + G_{15} group, the expression of TXNIP protein was higher significantly than in the G_1 group (at 24 and 48 h). Similarly, in the TAM + G_{15} group, there was a considerable increase in TXNIP protein compared to the TAM group (at 24 and 48 h). The concurrent treatment with both G_1 and TAM was ineffective in altering the protein expression of TXNIP at 24 and 48 h compared to each agent alone (Fig. 3D).

The effect of GPER induction or inhibition on miR-17-5P expression

The presence of certain microRNAs binding to complementary sequences in the 3´UTR of gene targets can impact the stability of mRNAs (28). In the TXNIP 3´UTR, two conserved binding sites for miR-17-5p have been identified (29). Additionally, IRE1α can degrade specific mRNAs or pre-miRNAs through RIDD activity. To confirm that IRE1α can affect TXNIP stability *via* miR-17-5P degradation, we examined the expression of miR-17-5P in the GPER/IRE1α/TXNIP signaling pathway after treatment with G_1,

TAM, and G_{15}. The results showed that there was no significant change in miR-17-5P expression, indicating that it is not affected by the GPER/IRE1α/TXNIP signaling pathway. Other pathways and factors are probably involved, which require further investigation (Fig. 4A).

The relevance between the GPER/IRE1α/TXNIP signaling pathway and chemotherapy resistance

In this study, to explore the potential relationship between GPER and the genes involved in chemotherapy resistance, MDA-MB231 cells were treated with G_1, TAM, and G_{15} for 24 and 48 h. The expression levels of P-glycoprotein (ABCB1) and multidrug resistance-associated protein-1 (MRP1/ ABCC1) were determined by qRT-PCR analyses. Interestingly, ABCB1 (Fig. 4B) and ABCC1 (Fig. 4C) genes were predominantly expressed in the MDA-MB231 cells after 24- and 48-treatment with G_1 and TAM. The chemotherapy resistance induced by G_1 and TAM could be restored by G_{15} in these cells. Pre-treatment of G_{15} for 24 and 48 h reduced the expression of resistance genes in G_1 + G_{15} and TAM + G_{15} groups compared to G_1 and TAM groups. When the cells were treated with G_1 and TAM simultaneously, the expression of ABCB1 and ABCC1 were elevated compared to both G_1 and TAM groups. The results indicated that after 48 h of treatment levels of ABCB1 mRNA markedly increased in the G_1, TAM, and G_1 + TAM groups when compared to 24-h treatment; in contrast, an elevation in ABCC1 expression was observed solely in the TAM and G_1 + TAM groups after 48 h.

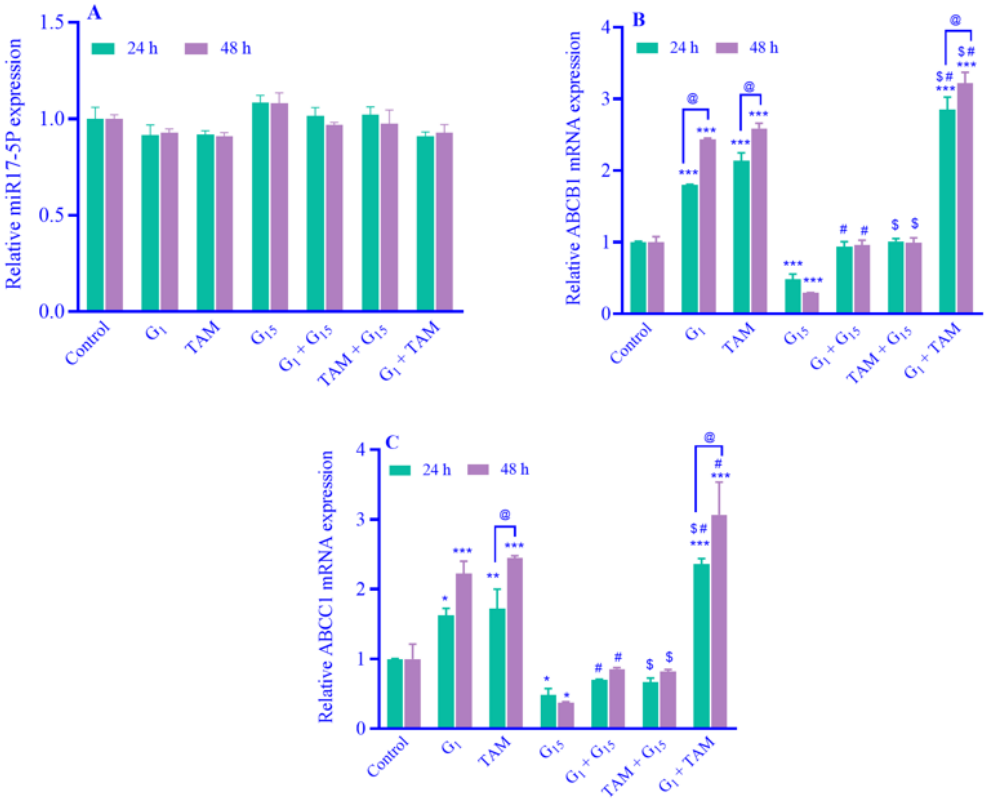

Fig. 4. Evaluating the relevance between the GPER/IRE1α/TXNIP signaling pathway and miR-17-5P, ABCB1, and ABCC1 gene expression in MDA-MB231 cells. MDA-MB231 cells were treated with G_1, TAM, G_{15}, G_1 + G_{15}, TAM + G_{15}, and G_1 + TAM at 24 and 48 h. Then, the relative expression of (A) miR-17-5P, (B) ABCB1, and (C) ABCC1 genes were assessed by qRT-PCR. Data represent the mean ± SD, n = 3. $^{*}P < 0.05$, $^{**}P < 0.01$, and $^{***}P < 0.001$ indicate significant differences compared to the control group; $^{\#}P < 0.05$ versus G_1 group; $^{\$}P < 0.05$ against TAM group; and $^{@}P < 0.05$ indicate significant differences between the designated groups. TAM, Tamoxifen; GPER, G-protein-coupled estrogen receptor; IRE, inositol-requiring enzyme; TXNIP, thioredoxin interacting protein; ABCB1, ATP binding cassette subfamily B member 1; ABCC1, ATP binding cassette subfamily C member 1.

The relevance between the GPER/IRE1α/TXNIP signaling pathway and apoptosis

To understand the relevance between the activated GPER/IRE1α/TXNIP signaling pathway and apoptosis in MDA-MB231 cells, we tested the effect of GPER induction or inhibition on cell apoptosis using flow cytometry. Treatment with G_1 and TAM did not inhibit the growth of MDA-MB-231 cells; however, G_{15} treatment increased apoptosis compared to the control group. Pre-treatment of cells with G_{15} increased apoptosis in the G_1 + G_{15} and TAM + G_{15} groups compared to the control group. Furthermore, we observed an induction of apoptosis in the G_1 + G_{15} group compared to the G_1 group and in the TAM + G_{15} group compared to the TAM group. There was a significant difference in apoptosis between the co-treatment with the G_1 + TAM group and the G_1 group alone, as well as the TAM group alone. The amount of apoptosis in cells is reported based on the sum of early apoptosis and late apoptosis ($Q_2 + Q_3$) (Fig. 5).

The relevance between the GPER/IRE1α/ TXNIP signaling pathway and cell migration

This study aimed to investigate the influence of activated or inhibited GPER signaling on the metastatic behavior of MDA-MB231 cells. As these cells are a highly aggressive type of breast cancer, we sought to determine if the metastatic capacity of MDA-MB231 cells was entirely or partially influenced by activated or inhibited GPER signaling. The wound-healing assay was utilized to evaluate the cell migration capability. As shown in Fig. 6A and B, the activation of the downstream GPER/IRE1α/ TXNIP signaling pathway by G_1/TAM significantly enhanced the migration ability of MDA-MB231 cells. Paradoxically, the cell-invasive ability of MDA-MB231 cells decreased with G_{15} treatment. Also, a significant difference was observed in G_1 + G_{15}, TAM + G_{15}, and G_1 + TAM groups compared to the control group. Compared to the G_1 group, the G_1+ G_{15} group exhibited a significant decrease in invasion ability in these cells. Similarly, the TAM + G_{15} group also exhibited a significant reduction in invasion ability compared to the TAM group (Fig. 6).

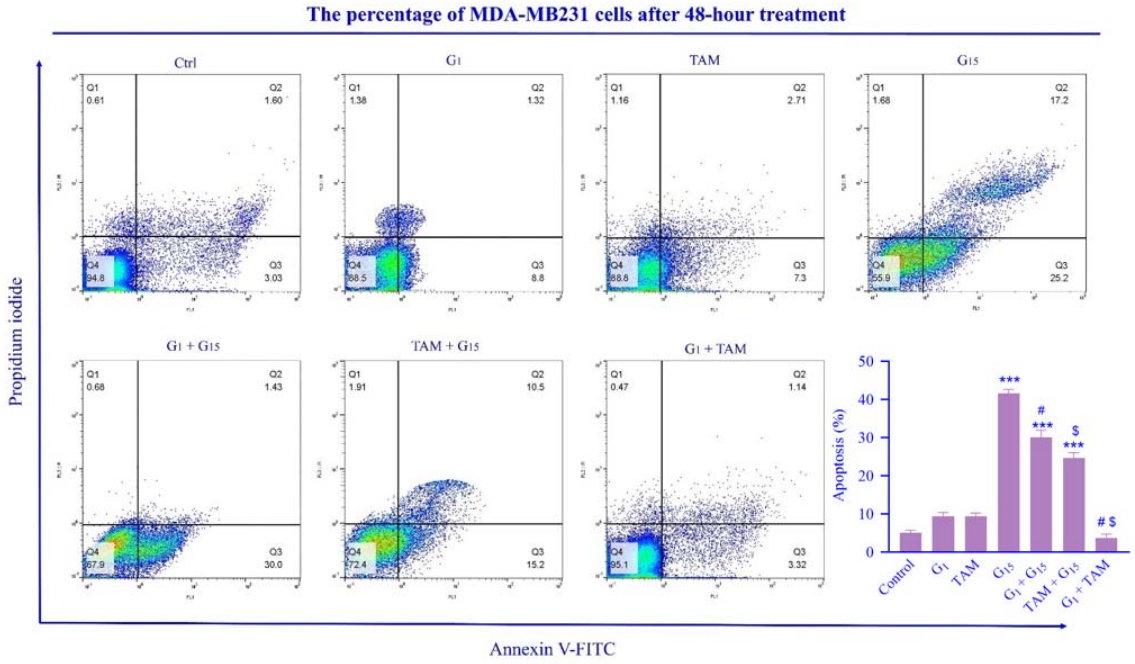

Fig. 5. Evaluating the relevance between the GPER/IRE1α/TXNIP signaling pathway and apoptosis in MDA-MB231 cells. The flow cytometry assay was used to assess cell death after 48 h of treatment with G_1, TAM, G_{15}, G_1 + G_{15}, TAM + G_{15}, and G_1 + TAM. The amount of apoptosis in cells is reported based on the sum of early and late apoptosis (Q2 + Q3). ***$P < 0.001$ indicates significant differences compared to the control group; $^{\#}P < 0.05$ versus G_1 group; $^{\$}P < 0.05$ in contrast to the TAM group. TAM, Tamoxifen; GPER, G-protein-coupled estrogen receptor; IRE, inositol-requiring enzyme; TXNIP, thioredoxin interacting protein.

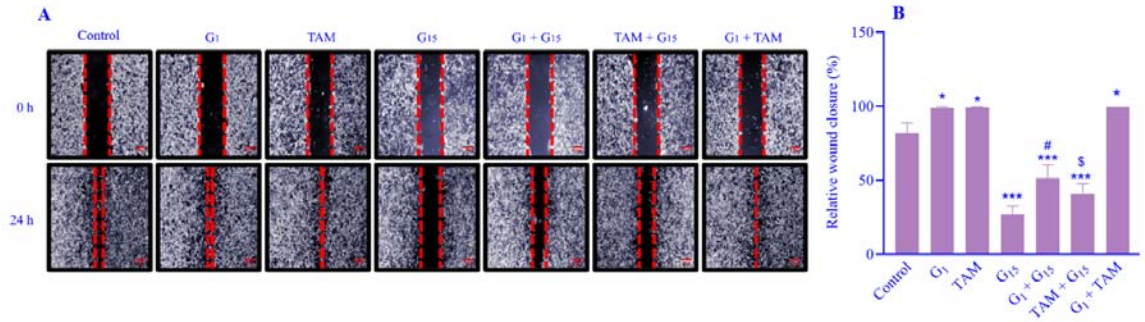

Fig. 6. Evaluating the relevance between the GPER/IRE1α/TXNIP signaling pathway and cell migration in MDA-MB231 cells. (A) The cell migration ability was determined using the wound-healing assay after 24 h of treatment with G_1, TAM, G_{15}, $G_1 + G_{15}$, TAM + G_{15}, and G_1 + TAM. (B) The data represent means ± SD, n = 3. *$P < 0.05$ and ***$P < 0.001$ indicate significant differences compared to the control group; $^{\#}P < 0.05$ versus G_1 group; $^{\$}P < 0.05$ in contrast to the TAM group).

DISCUSSION

TNBC accounts for 15% of all breast cancer cases. It is known for its aggressive nature, early recurrence, and poor prognosis. Due to its unique molecular characteristics and biological diversity, TNBC has fewer treatment options compared to other breast cancer types. Therefore, researchers have concentrated much of their attention on estrogen receptors, particularly GPER. GPER mediates estrogen action in various pathophysiological conditions, including cancer. When estrogen binds to GPER, it initiates a cascade of signaling events within the cell, affecting processes such as cell growth, proliferation, survival, and migration (30). While some studies suggest GPER's involvement in breast cancer development and progression (8,10), others propose a potential tumor-suppressive role for GPER (12,13,31). Therefore, understanding GPER's role in breast cancer biology holds promise for the development of more effective treatment strategies, particularly for patients with hormone receptor-positive disease.

In this research, we found that the induction of GPER using G_1 and TAM can be associated with metastasis and drug resistance through the GPER/IRE1α/TXNIP pathway in MDA-MB-231 cells. We observed that following GPER induction, the expression of IRE1α significantly increased, while there was no significant change in miR-17-5P expression. Consequently, the stability of TXNIP *via* miR-17-5P cleavage was unaffected, resulting in reduced TXNIP expression in gene and protein levels. According to the role of IRE1α, one of the reasons for the pro-survival response of the UPR in the MDA-MB231 cell line is the induction of the GPER/IRE1α/TXNIP signaling pathway. This pathway leads to the splicing of XBP1, a potent transcription factor, through IRE1's endoribonuclease activity. XBP1 then aids in the destruction of misfolded proteins through the activation of endoplasmic-reticulum-associated protein degradation and promotes proper protein folding by increasing chaperone levels, ultimately protecting the survival of cancer cells.

TXNIP is a strong suppressor of tumors (32) and its expression is significantly lower in both human breast cancer tissues and animal mammary tumors compared to normal tissues. This decrease in TXNIP expression was found to be associated with tumor progression. Researchers also observed that tumors with high proliferative activity, as indicated by high Ki_{67} labeling indexes and low p27 expression, were more likely to have reduced levels of TXNIP protein. In laboratory and animal studies, the knockdown of TXNIP resulted in increased growth of breast cancer cells, along with reduced p27 levels and increased glucose transporter-1 expression. Additionally, the expression of TXNIP decreased when estrogen receptor signaling was activated by estradiol, but increased when the receptor was blocked by the antiestrogen fulvestrant. Furthermore, knocking down TXNIP in breast cancer cells reduced the inhibitory effect of fulvestrant on cell growth (19). Similar results were observed

in our study about the MDA-MB231 cell line. Although IRE1α could not affect the expression of miR-17-5P through its RIDD activity, the expression of TXNIP decreased following the induction of the GPER/IRE1α signaling pathway and led to cell survival. Probably, IRE1α affects the expression of TXNIP through other pathways. A study identified c-Myc as a novel direct downstream target of IRE1α/XBP1 to regulate natural killer cell proliferation. Either genetic removal or pharmaceutical inhibition of IRE1α resulted in the downregulation of c-Myc, and natural killer cells with reduced c-Myc expression mimicked the effects of IRE1α/XBP1 deficiency. Thus, there is a reciprocal relationship between IRE1α and c-Myc activation (33). Interestingly, c-Myc reduces TXNIP expression by binding to its promoter's E-box region. The association between the $c\text{-}Myc_{high}/TXNIP_{low}$ gene signature and unfavorable clinical outcomes is observable solely in TNBC, not in other types of breast cancer. Therefore, these findings demonstrate that IRE1α reduces TXNIP gene and protein expression through c-Myc activation, exacerbating the aggressive clinical features of MDA-MB231 cells, such as increased cell proliferation and migration, and notably decreasing cell death (34).

Our results showed upon GPER induction in MDA-MB231 cells, a notable reduction in apoptosis was observed. Importantly, these effects were reversed when cells were treated with G_{15}. The decrease of apoptosis in the studied cell line is related to the expression level of TXNIP protein. Xu and colleagues found that over 67.1 months, there was a notable decrease in distant metastasis-free survival in patients with high GPER expression. Their Kaplan-Meier analysis revealed a significant association between GPER expression and distant metastasis-free survival in TNBC patients. Additionally, high GPER levels were connected to poorer survival outcomes in patients with lymph node metastasis, TNM stage III, and nuclear grade G3 tumors. These findings offer new perspectives on how GPER influences estrogen-related cancer development in TNBC, suggesting a potential approach for endocrine therapy in this type of breast cancer (35). Lin *et al.*'s findings align with our study, demonstrating a significant decrease in TXNIP expression in hepatocellular carcinoma tissues. Additionally, they found that TXNIP overexpression suppressed hepatocellular carcinoma cell proliferation and induced apoptosis by promoting mitochondrial-mediated reactive oxygen species (ROS) generation and activating MAPK pathways (36). Therefore, the expression of the gene and protein of TXNIP in cancer cells has a direct relationship with the level of apoptosis. TXNIP can increase the amount of apoptosis by inhibiting thioredoxin and increasing ROS generation and the MAPK pathway and p27 activation (19,36).

One of the primary causes of chemoresistance is the overexpression of multidrug resistance transporters (37). Our study indicated that upon GPER induction in MDA-MB231 cells, there was a notable increase in cell migration and the expression of genes related to drug resistance. Chen *et al.* reported that inhibiting c-Myc could induce the upregulation of TXNIP in drug-resistant TNBC cells. The increased TXNIP levels subsequently enhance the accumulation of DNA damage dependent on ROS, thereby reducing chemotherapy resistance in TNBC (38). Yu *et al*. discovered a notable increase in GPER and ATP-binding cassette super-family G member-2 (ABCG2) expression in TAM-resistant ER^+ metastases compared to primary tumors, with metastatic patients showing a plasma membrane expression pattern of these proteins. They identified that downstream GPER/EGFR/ERK and GPER/EGFR/AKT signaling pathways regulated ABCG2 expression and membrane localization in TAM-resistant breast cancer cells (MCF-7R) (39). Logue *et al.* demonstrated that the chemotherapy agent paclitaxel increases the activity of IRE1α RNase, resulting in the expansion of tumor-initiating cells. In a xenograft mouse model of TNBC, inhibiting IRE1α RNase activity enhances the tumor-suppressive effects of paclitaxel and prolongs the delay in tumor relapse following therapy. The authors also observed a link between IRE1α RNase activity and the production of pro-inflammatory factors in TNBC cells (40).

In the study conducted by Yu *et al*., the effects of E_2, TAM, and G_1 on MDA-MB-468 and MDA-MB-436 cells were examined. Specifically, the estrogen/GPER/ERK pathway, cell cycle, and Bcl-2 and c-fos genes were analyzed. The results indicated that treatment with E_2, TAM, and G_1 resulted in a rapid activation of p-ERK1/2. This signaling pathway was found to play a role in promoting cell growth, survival, migration, and invasion by increasing the expression of cyclin A, cyclin D_1, Bcl 2, and c-fos. These proteins are involved in regulating the cell cycle, inhibiting apoptosis, and promoting proliferation, respectively (22). Consistent with prior research, we observed that G_1/TAM activated the downstream GPER/IRE1α/TXNIP signaling pathway, resulting in heightened cell migration and upregulation of ABCB1 and ABCC1 gene expression. Importantly, all of these effects were reversed upon blocking GPER using G_{15}. While MTT results showed that low concentrations of G_1 and TAM exhibited limited cytotoxic effects, they slightly reduced cell growth (by around 16-19% at the studied concentrations) but significantly increased cell migration. Adhesion molecules are believed to be one of the reasons for the discrepancy between cell growth and migration in MDA-MB231 cells after treatment with G_1 and TAM. In 2005, Moh *et al.* for the first time identified an immunoglobulin superfamily cell adhesion molecule hepaCAM that can suppress cancer cell growth and yet induce migration (41).

Re-expression of hepaCAM in HepG2 (41) and MCF7 cells (42) inhibited colony formation, induced cell cycle arrest at the G2/M phase, triggered cellular senescence, and slowed cell proliferation *via* a p53/p21-dependent pathway. Additionally, hepaCAM expression enhanced ell-extracellular matrix adhesion and cell migration in these cells (43). Almost concurrently, the type I membrane protein receptor carcinoembryonic antigen-related cell adhesion molecule 1 (CEACAM1) was verified to co-function as a tumor suppressor and invasion promoter (44). Ebrahimnejad *et al.* have demonstrated that melanoma cell invasion and migration are made more effective by exogenous expression of CEACAM1 (45). The ability of CEACAM to co-stimulate tumor suppression and invasion was finally established by Liu *et al.* (46). To date, the reason and mechanism responsible for this exceptional phenomenon remain unclear. Nevertheless, the emergence of these intriguing cell adhesion molecules with conflicting roles may open a new chapter to the biological significance of cell adhesion molecules (47).

Our findings provide new insights into the possible connection between chemotherapy resistance and GPER. Nevertheless, further exploration of alternative pathways in this field is necessary. Targeting the GPER/IRE1α/TXNIP signaling axis, along with the ABCB1 and ABCC1 genes, may present a promising strategy for overcoming chemotherapy resistance in patients with advanced breast cancer.

Overall, investigating the relationship between the GPER pathway and UPR in triple-negative breast cancer, and determining whether the induction or inhibition of this pathway benefits or hinders cancer progression, is one of the strengths of this study compared to previous research. Additionally, we examined the impact of the GPER/IRE1α/miR-17-5P/TXNIP pathway on cell behaviors, such as apoptosis, migration, and cell resistance, which have not been assessed previously. Due to a lack of financial resources, there are some weaknesses compared to previous studies. For instance, there was no investigation of the cell proliferation index (Ki67), the expression of genes and proteins related to apoptosis (*e.g.* BAX, BCL-2, c-Myc, P53), genes involved in angiogenesis (VEGF and KDR), and no studies on onco-miRs or other tumor suppressor miRs involved in breast cancer. Furthermore, we did not utilize siRNAs for GPER silencing or explore the downstream pathways associated with it.

CONCLUSION

Our findings illustrate that G_1 and TAM induction of GPER leads to the upregulation of IRE1α. Through its endoribonuclease activity, IRE1α cleaves XBP1, resulting in heightened migration, drug resistance, and ultimately, enhanced survival of the MDA-MB231 cell

line. Moreover, GPER induction decreases TXNIP gene and protein expression, leading to diminished apoptosis. In summary, our study provides a comprehensive understanding of non-genomic signaling through GPER in the MDA-MB231 cell line. Inhibiting the GPER/IRE1α/TXNIP pathway holds promise as a strategy to improve treatment outcomes and enhance chemotherapy sensitivity in TNBC cancer patients. Nonetheless, further research, including prospective clinical trials, is required to validate these findings.

Acknowledgments

This research was funded by the Kerman University of Medical Sciences (KUMS) (grant No. 00/10/60/582) and the Molecular Medicine Research Center (MMRC) at the Rafsanjan University of Medical Sciences (RUMS) through Grant No. 31/20/1/99242 in Iran. Ethical approval was obtained under the code IR.KMU.AH.REC.1399.187. The authors would like to express their appreciation to both universities for providing the essential equipment for this study.

Conflict of interest statement

The authors declared no conflicts of interest in this study.

Authors' contributions

M. Mohammad-Sadeghipour participated in the conception and design of the study, drafting, acquisition of data, analysis, and interpretation of the data, M.H. Nematollahi contributed to the conception and design of the study, supervision, and revising the article; H. Ahmadinia collaborated in statistical analysis; M.R. Hajizadeh and M. Mahmoodi were responsible for the conception and design the study, project administration, revising the article. The finalized article was read and approved by all authors.

REFERENCES

1. Settacomkul R, Sangpairoj K, Phuagkhaopong S, Meemon K, Niamnont N, Sobhon P, *et al*. Ethanolic extract of *Halymenia durvillei* induced G2/M arrest and altered the levels of cell cycle regulatory proteins of MDA-MB-231 triple-negative breast cancer cells. Res Pharm Sci. 2023;18(3):279-291. DOI: 10.4103/1735-5362.371584.
2. Kao J, Salari K, Bocanegra M, Choi YL, Girard L, Gandhi J, *et al*. Molecular profiling of breast cancer cell lines defines relevant tumor models and provides a resource for cancer gene discovery. PLoS One. 2009;4(7):e6146,1-16. DOI: 10.1371/journal.pone.0006146.
3. Vyshnavi H, Namboori K. Identifying potential ligand molecules EGFR mediated TNBC targeting the kinase domain-identification of customized drugs through *in silico* methods. Res Pharm Sci. 2023;18(2):121-137. DOI: 10.4103/1735-5362.367792.
4. Derakhshan F, Reis-Filho JS. Pathogenesis of triple-negative breast cancer. Annu Rev Pathol. 2022;17:181-204. DOI: 10.1146/annurev-pathol-042420-093238.
5. Li Y, Zhang H, Merkher Y, Chen L, Liu N, Leonov S, *et al*. Recent advances in therapeutic strategies for triple-negative breast cancer. J Hematol Oncol. 2022;15(1):121,1-30. DOI: 10.1186/s13045-022-01341-0.
6. Girgert R, Emons G, Gründker C. Estrogen signaling in ERα-negative breast cancer: ERβ and GPER. Front endocrinol. 2019;9:781,1-12. DOI: 10.3389/fendo.2018.00781.
7. Han N, Heublein S, Jeschke U, Kuhn C, Hester A, Czogalla B, *et al*. The G-protein-coupled estrogen receptor (GPER) regulates trimethylation of histone H3 at lysine 4 and represses migration and proliferation of ovarian cancer cells *in vitro*. Cells. 2021;10(3):619,1-23. DOI: 10.3390/cells10030619.
8. Ignatov T, Claus M, Nass N, Haybaeck J, Seifert B, Kalinski T, *et al*. G-protein-coupled estrogen receptor GPER-1 expression in hormone receptor-positive breast cancer is associated with poor benefit of tamoxifen. Breast Cancer Res Treat. 2019;174(1):121-127. DOI: 10.1007/s10549-018-5064-8.
9. Lei B, Peng W, Xu G, Wu M, Wen Y, Xu J, *et al*. Activation of G protein-coupled receptor 30 by thiodiphenol promotes proliferation of estrogen receptor alpha-positive breast cancer cells. Chemosphere. 2017;169:204-211. DOI: 10.1016/j.chemosphere.2016.11.066.
10. Vivacqua A, Sebastiani A, Miglietta AM, Rigiracciolo DC, Cirillo F, Galli GR, *et al*. MiR-338-3p is regulated by estrogens through GPER in breast cancer cells and cancer-associated fibroblasts (CAFs). Cells. 2018;7(11):203,1-19. DOI: 10.3390/cells7110203.
11. Liang S, Chen Z, Jiang G, Zhou Y, Liu Q, Su Q, *et al*. Activation of GPER suppresses migration and angiogenesis of triple negative breast cancer via inhibition of NF-κB/IL-6 signals. Cancer lett. 2017;386:12-23. DOI: 10.1016/j.canlet.2016.11.003.
12. Vo DKH, Hartig R, Weinert S, Haybaeck J, Nass N. G-protein-coupled estrogen receptor (GPER)-specific agonist G1 induces ER stress leading to cell death in MCF-7 cells. Biomolecules. 2019;9(9):503,1-21. DOI: 10.3390/biom9090503.

13. Weissenborn C, Ignatov T, Poehlmann A, Wege AK, Costa SD, Zenclussen AC, *et al*. GPER functions as a tumor suppressor in MCF-7 and SK-BR-3 breast cancer cells. J Cancer Res Clin Oncol. 2014;140(4):663-671.
DOI: 10.1007/s00432-014-1598-2.
14. Sisinni L, Pietrafesa M, Lepore S, Maddalena F, Condelli V, Esposito F, *et al*. Endoplasmic reticulum stress and unfolded protein response in breast cancer: the balance between apoptosis and autophagy and its role in drug resistance. Int J Mol Sci. 2019;20(4):857,1-17.
DOI: 10.3390/ijms20040857.
15. Adams CJ, Kopp MC, Larburu N, Nowak PR, Ali MMU. Structure and molecular mechanism of ER stress signaling by the unfolded protein response signal activator IRE1. Front Mol Biosci. 2019;6:11,1-12.
DOI: 10.3389/fmolb.2019.00011.
16. Barua D, Gupta A, Gupta S. Targeting the IRE1-XBP1 axis to overcome endocrine resistance in breast cancer: opportunities and challenges. Cancer Lett. 2020;486:29-37.
DOI: 10.1016/j.canlet.2020.05.020.
17. Oslowski CM, Urano F. Measuring ER stress and the unfolded protein response using mammalian tissue culture system. Methods Enzymol. 2011;490:71-92.
DOI: 10.1016/B978-0-12-385114-7.00004-0.
18. Wu J, He GT, Zhang WJ, Xu J, Huang QB. IRE1α signaling pathways involved in mammalian cell fate determination. Cell Physiol Biochem. 2016;38(3):847-858.
DOI: 10.1159/000443039.
19. Park JW, Lee SH, Woo GH, Kwon HJ, Kim DY. Downregulation of TXNIP leads to high proliferative activity and estrogen-dependent cell growth in breast cancer. Biochem Biophys Res Commun. 2018;498(3):566-572.
DOI: 10.1016/j.bbrc.2018.03.020.
20. Lee JH, Jeong J, Jeong EM, Cho SY, Kang JW, Lim J, *et al*. Endoplasmic reticulum stress activates transglutaminase 2 leading to protein aggregation. Int J Mol Med. 2014;33(4):849-855.
DOI: 10.3892/ijmm.2014.1640.21. Wei W, Chen ZJ, Zhang KS, Yang XL, Wu YM, Chen XH, *et al*. The activation of G protein-coupled receptor 30 (GPR30) inhibits proliferation of estrogen receptor-negative breast cancer cells *in vitro* and *in vivo*. Cell Death Dis. 2014;5(10):e1428,1-12.
DOI: 10.1038/cddis.2014.398.
22. Yu T, Liu M, Luo H, Wu C, Tang X, Tang S, *et al*. GPER mediates enhanced cell viability and motility via non-genomic signaling induced by 17β-estradiol in triple-negative breast cancer cells. J Steroid Biochem Mol Biol. 2014;143:392-403.
DOI: 10.1016/j.jsbmb.2014.05.003.
23. Wang LJ, Han SX, Bai E, Zhou X, Li M, Jing GH, *et al*. Dose-dependent effect of tamoxifen in tamoxifen-resistant breast cancer cells via stimulation by the ERK1/2 and AKT signaling pathways. Oncol Rep. 2013;29(4):1563-1569.
DOI: 10.3892/or.2013.2245.
24. Shahali A, Ghanadian M, Jafari SM, Aghaei M. Mitochondrial and caspase pathways are involved in the induction of apoptosis by nardosinen in MCF-7 breast cancer cell line. Res Pharm Sci. 2018;13(1):12-21.
DOI: 10.4103/1735-5362.220963.
25. Liu L, Liu S, Luo H, Chen C, Zhang X, He L, *et al*. GPR30-mediated HMGB1 upregulation in CAFs induces autophagy and tamoxifen resistance in ERα-positive breast cancer cells. Aging (Albany NY). 2021;13(12):16178-16197.
DOI: 10.18632/aging.203145.
26. Samii B, Jafarian A, Rabbani M, Zolfaghari B, Rahgozar S, Pouraboutaleb E. The effects of Astragalus polysaccharides, tragacanthin, and bassorin on methotrexate-resistant acute lymphoblastic leukemia. Res Pharm Sci. 2023;18(4):381-391.
DOI: 10.4103/1735-5362.378085.
27. Liu C, Liao Y, Fan S, Fu X, Xiong J, Zhou S, *et al*. G-protein-coupled estrogen receptor antagonist G15 decreases estrogen-induced development of non-small cell lung cancer. Oncol Res. 2019;27(3):283-292.
DOI: 10.3727/096504017x15035795904677.
28. Masoudi F, Sharifi MR, Pourfarzam M. Investigation of the relationship between miR-33a, miR-122, erythrocyte membrane fatty acids profile, and serum lipids with components of metabolic syndrome in type 2 diabetic patients. Res Pharm Sci. 2022;17(3):242-251.
DOI: 10.4103/1735-5362.343078.
29. Coucha M, Mohamed IN, Bartasis ML, El-Remessy AB. High fat diet dysregulates microRNA-17-5p and enhances retinal TXNIP expression: role of ER-stress. Investig Ophthalmol Vis Sci. 2015;56(7):2391.
30. Luo H, Yang G, Yu T, Luo S, Wu C, Sun Y, *et al*. GPER-mediated proliferation and estradiol production in breast cancer-associated fibroblasts. Endocr Relat Cancer. 2014;21(2):355-369.
DOI: 10.1530/erc-13-0237.
31. Shen Y, Yang F, Zhang W, Song W, Liu Y, Guan X. The androgen receptor promotes cellular proliferation by suppression of G-protein coupled estrogen receptor signaling in triple-negative breast cancer. Cell Physiol Biochem. 2017;43(5):2047-2061.
DOI: 10.1159/000484187.
32. Choi EH, Park SJ. TXNIP: a key protein in the cellular stress response pathway and a potential therapeutic target. Exp Mol Med. 2023;55(7): 1348-1356.
DOI: 10.1038/s12276-023-01019-8.
33. Dong H, Adams NM, Xu Y, Cao J, Allan DSJ, Carlyle JR, *et al*. The IRE1 endoplasmic reticulum stress sensor activates natural killer cell immunity in part by regulating c-Myc. Nat Immunol. 2019;20(7):865-878.
DOI: 10.1038/s41590-019-0388-z.
34. Shen L, O'Shea JM, Kaadige MR, Cunha S, Wilde BR, Cohen AL, *et al*. Metabolic reprogramming in triple-negative breast cancer through Myc

suppression of TXNIP. Proc Natl Acad Sci U S A. 2015;112(17):5425-5430.
DOI: 10.1073/pnas.1501555112.
35. Xu T, Ma D, Chen S, Tang R, Yang J, Meng C, *et al*. High GPER expression in triple-negative breast cancer is linked to pro-metastatic pathways and predicts poor patient outcomes. NPJ Breast Cancer. 2022;8(1):100,1-11.
DOI: 10.1038/s41523-022-00472-4.
36. Li J, Yue Z, Xiong W, Sun P, You K, Wang J. TXNIP overexpression suppresses proliferation and induces apoptosis in SMMC7221 cells through ROS generation and MAPK pathway activation. Oncol Rep. 2017;37(6):3369-3376.
DOI: 10.3892/or.2017.5577.
37. Rajaei N, Rahgouy G, Panahi N, Razzaghi-Asl N. Bioinformatic analysis of highly consumed phytochemicals as P-gp binders to overcome drug-resistance. Res Pharm Sci. 2023;18(5):505-516.
DOI: 10.4103/1735-5362.383706.
38. Chen Y, Feng X, Yuan Y, Jiang J, Zhang P, Zhang B. Identification of a novel mechanism for reversal of doxorubicin-induced chemotherapy resistance by TXNIP in triple-negative breast cancer via promoting reactive oxygen-mediated DNA damage. Cell Death Dis. 2022;13(4):338,1-13.
DOI: 10.1038/s41419-022-04783-z.
39. Yu T, Cheng H, Ding Z, Wang Z, Zhou L, Zhao P, *et al*. GPER mediates decreased chemosensitivity *via* regulation of ABCG2 expression and localization in tamoxifen-resistant breast cancer cells. Mol Cell Endocrinol. 2020;506:110762,1-12.
DOI: 10.1016/j.mce.2020.110762.
40. Logue SE, McGrath EP, Cleary P, Greene S, Mnich K, Almanza A, *et al.* Inhibition of IRE1 RNase activity modulates the tumor cell secretome and enhances response to chemotherapy. Nat Commun. 2018;9(1):3267,1-15.
DOI: 10.1038/s41467-018-05763-8.
41. Moh MC, Lee LH, Shen S. Cloning and characterization of hepaCAM, a novel Ig-like cell adhesion molecule suppressed in human hepatocellular carcinoma. J Hepatol. 2005;42(6): 833-841.
DOI: 10.1016/j.jhep.2005.01.025.
42. Moh MC, Zhang T, Lee LH, Shen S. Expression of hepaCAM is downregulated in cancers and induces senescence-like growth arrest via a p53/p21-dependent pathway in human breast cancer cells. Carcinogenesis. 2008;29(12):2298-2305.
DOI: 10.1093/carcin/bgn226.
43. Moh MC, Zhang C, Luo C, Lee LH, Shen S. Structural and functional analyses of a novel Ig-like cell adhesion molecule, hepaCAM, in the human breast carcinoma MCF7 cells. J Biol Chem. 2005;280(29):27366-27374.
DOI: 10.1074/jbc.M500852200.
44. Nittka S, Böhm C, Zentgraf H, Neumaier M. The CEACAM1-mediated apoptosis pathway is activated by CEA and triggers dual cleavage of CEACAM1. Oncogene. 2008;27(26):3721-3728.
DOI: 10.1038/sj.onc.1211033.
45. Ebrahimnejad A, Streichert T, Nollau P, Horst AK, Wagener C, Bamberger AM, *et al*. CEACAM1 enhances invasion and migration of melanocytic and melanoma cells. Am J Pathol. 2004;165(5): 1781-1787.
DOI: 10.1016/s0002-9440(10)63433-5.
46. Liu W, Wei W, Winer D, Bamberger AM, Bamberger C, Wagener C, *et al.* CEACAM1 impedes thyroid cancer growth but promotes invasiveness: a putative mechanism for early metastases. Oncogene. 2007;26(19):2747-2758.
DOI: 10.1038/sj.onc.1210077.
47. Moh MC, Shen S. The roles of cell adhesion molecules in tumor suppression and cell migration. Cell Adh Migr. 2009;3(4):334-336.
DOI: 10.4161/cam.3.4.9246.